

Synthesis of Niobium Boride Nanoparticle by RF Thermal Plasma

Yingying Cheng, Sooseok Choi, and Takayuki Watanabe

Dept. Environmental Chemistry and Engineering, Tokyo Institute of Technology,
Yokohama, Japan

E-mail: watanabe@chemenv.titech.ac.jp

Abstract. Experimental study has been conducted to investigate the formation mechanism of transition metal boride nanoparticles in radio frequency thermal plasmas. The effect of nucleation temperature on the synthesis of niobium boride nanoparticles was investigated. The operating condition of powder feed rate plays an important role in the synthesis of boride nanoparticles. The mass fraction of niobium boride in the product was decreased with increasing powder feed rate. The main reason is that the evaporation time of niobium is long and the existence area of evaporated niobium is extended along with the thermal plasma flame at high powder feed rate. The diameter of the product increases along with the increase of powder feed rate due to increased monomer density in the plasma. In addition, high melting and boiling temperatures of niobium leads to high mass fraction over 96% of niobium boride in the collecting filter.

1. Introduction

Radio frequency (RF) thermal plasmas has many unique advantages including high enthalpy, high chemical reactivity, large plasma volume, long residence time, and selective oxidation or reduction atmosphere according to the required chemical reactions. The high temperature of thermal plasma enables the evaporation of a large amount of raw materials even with high melting and boiling temperatures [1-3]. The formation of nanoparticles in supersaturated state by homogeneous nucleation and heterogeneous condensation can be accomplished due to the rapid quenching rate in the tail flame [4-7]. Furthermore, it is available to synthesize nanoparticles with high purity by RF thermal plasma, because the thermal plasma is generated in the torch without an internal electrode.

Niobium borides are recognized as potential candidates for the application of high-temperature structural materials due to their excellent properties. Attractive properties of niobium borides are high melting temperature, high mechanical strength, high thermal and electrical conductivity, and excellent chemical stability [8]. The RF thermal plasma which can provide very high temperature without oxygen is a promising alternative to conventional methods in the synthesis of niobium boride nanoparticles.

In Nb-B system, the niobium with low saturation vapor pressure has high nucleation temperature compared with that of boron with relatively high saturation vapor pressure. As a result, the formation mechanism of niobium boride is different from that in Ti-B system where boron has lower saturation vapor pressure than titanium. In Ti-B system, boron nucleates first at the upstream region of thermal plasma flow, followed by the condensation of titanium monomers on boron nuclei. Since, boron nuclei on the liquid state have relatively wide temperature region, titanium boride are easy to fabricate. On



the other hand, niobium vapor with low saturation vapor pressure reach supersaturation state first and starts to nucleate in Nb-B system. The nucleation temperature is a critical factor for the synthesis of boride nanoparticles in the RF thermal plasma [10].

The purpose of this study is to examine the effect of nucleation temperature on the synthesis of niobium boride nanoparticles in the RF thermal plasma. The experiments were carried out with controlling the powder feed rate, because it changes nucleation temperatures of niobium and boron which play an important role in the formation of niobium boride nanoparticles in the RF thermal plasma. The nanoparticle products collected from the inner wall of the reaction chamber and the collection filter were compared in terms of phase composition and crystalline size based on X-ray diffractometry (XRD).

2. Experimental Procedure

The schematic apparatus of RF thermal plasma system for the production of boride nanoparticles is shown in figure 1. The system consists of a plasma torch, a reaction chamber, a particle collection filter, and a power supply. The plasma torch is composed of a water-cooled quartz tube and a water-cooled induction coil (3 turns), coupling its electromagnetic energy to the plasma at a frequency of 4 MHz. The feeding powders were niobium (particle size: 20 μm , purity: 98%, Kojundo Chemical Laboratory Co. Ltd., Japan) and crystalline boron (particle size: 45 μm , purity: 99%, Kojundo Chemical Laboratory Co. Ltd., Japan). Niobium and boron particles were mixed at the fixed initial molar composition before they were injected into the RF thermal plasma through the powder feeder.

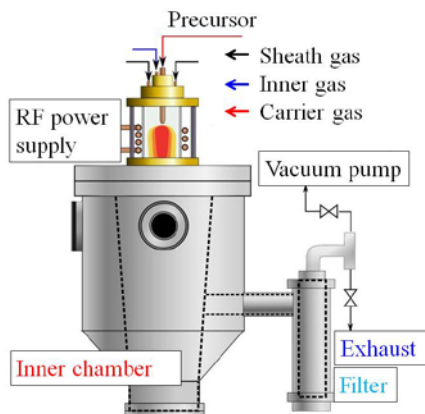


Figure 1. Experimental set-up of RF thermal plasma for the synthesis of metal boride nanoparticles.

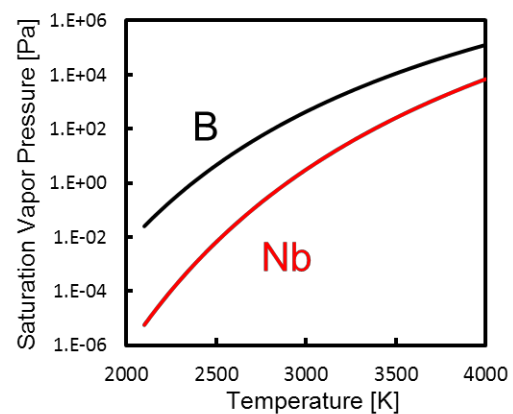


Figure 2. Relationship between saturation vapour pressures and temperature in Nb-B system.

After the precursors were introduced into the plasma region with argon carrier gas, they were instantaneously evaporated due to the very high enthalpy of the RF thermal plasma. Therefore, niobium boride nanoparticles are synthesized from the gas phase.

The operating conditions are summarized in Table 1. Argon was introduced as the carrier gas of 3 L/min, the inner gas of 5 L/min, and the sheath gas of 60 L/min. Helium of 5 L/min was also used as the sheath gas. The sheath gases were injected from the outer slots of the plasma torch located between the injection tube and the quartz tube to protect the inner surface of the quartz tube and to stabilize the plasma. The powder feed rate was 0.2, 0.5, and 1.0 g/min and the molar content of boron in the feeding powder was controlled from 33.3 to 80.0 at.%. The RF plasma was operated at the fixed input power of 30.4 kW under atmospheric pressure.

The synthesized nanoparticles were characterized for phase identification by XRD (MXP3TA, Mac Science). The crystalline size was calculated from the full widths at the half maximum (FWHM) of the most intensive diffractions according to the Scherrer's equation. Quantitative phase analysis by using

XRD data was carried out based on the adiabatic method [9]. This method evaluates the mass fraction of each phase from the relative intensity of the diffraction peak of product. The mass fraction of X phase can be calculated by following equation (1)

$$W_X = \frac{I_X}{K_A^X \sum_{X=A}^N \frac{I_X}{K_A^X}} = \frac{I_X}{K_{Ti}^X \cdot \left(\frac{I_{Nb}}{K_{Nb}^{Nb}} + \frac{I_{NbB}}{K_{Nb}^{NbB}} + \frac{I_{NbB_2}}{K_{Nb}^{NbB_2}} \right)} \quad (1)$$

where, X ($= Nb, NbB, NbB_2$) denotes each phase in the product. I_X presents the intensity of X phase in the product from the XRD spectrum. K_A^X is the ratio of the reference intensity ratio (RIR) values of X phase to that of the reference phase A , *i.e.*, $K_A^X = RIR_X/RIR_A$. In the experimental measurement of Nb-B system, three peaks for Nb, NbB and NbB₂ were identified in XRD spectrum, and Nb was selected as the reference materials. Based on the powder diffraction file cards, RIR values for Nb, NbB and NbB₂ are determined to be 19.34, 5.43, and 8.26, respectively.

Table 1 Operating condition for the synthesis of niobium boride nanoparticles

Process parameters	Value
Sheath gas and flow rate	Ar-He (60:5) 65 L/min
Inner gas and flow rate	Ar 5 L/min
Carrier gas and flow rate	Ar 3 L/min
Plasma power	30.4 kW
Reactor pressure	101.3 kPa
Frequency	4 MHz
Powder Feed rate	0.2-1.0 g/min
Boron molar content in feeding powder	33.3-80.0 at. %

3. Nucleation Temperature and Formation Mechanism

The nucleation temperatures of niobium and boron play an important role in the controlled synthesis of niobium boride nanoparticles in the RF thermal plasma. Materials with high saturation vapour pressure leads to low nucleation temperature, while lower saturation vapour pressure results in relatively higher nucleation temperature. Figure 2 shows the saturation vapour pressure according to the temperature in Nb-B system. The nucleation temperatures of niobium and boron at the critical saturation ratio are presented in figure 3. The nucleation temperature was calculated by equation (2) for the nucleation rate J . The particle formation was observed experimentally at $J = 1.0 \text{ cm}^{-3} \text{ s}^{-1}$ [11].

$$J = \frac{\beta_{11} N_s^2 S}{12} \sqrt{\frac{\Theta}{2\pi}} \exp \left[\Theta - \frac{4\Theta^3}{27(\ln S)^2} \right] \quad (2).$$

Here, N_s is the equilibrium saturation monomer concentration at temperature T , and it is estimated by the saturation vapour pressure. β_{11} , S , and Θ are the collision frequency function between monomers, the saturation ratio, and the dimensionless surface tension, respectively.

The formation mechanism of boride nanoparticles is based on the nucleation temperature of the constituent components. After the precursors are injected into the plasma, they are instantaneously evaporated due to the high temperature. The vapours are transported with the plasma flow to the reaction chamber where the plasma temperature decreases rapidly. The saturation vapour pressure of evaporated precursors decreases drastically along with the temperature decrease and will fall below their partial pressures in plasma. At this moment, the vapour of raw materials reaches their

supersaturation state. The supersaturation of vapours leads to the production of nuclei by homogeneous nucleation. In Nb-B system, niobium vapour is supersaturated first due to its lower saturation vapour pressure than that of boron. Simultaneously, the nucleation of niobium takes place and niobium nuclei are generated on molten state. The partial pressure of niobium vapour decreases rapidly, which is attributed to the vapour consumption by the nanoparticles growth with homogeneous nucleation and heterogeneous condensation. Then the co-condensation of boron and niobium occurs dominantly on the surface of the niobium nuclei. The partial pressure of boron vapour decreases by heterogeneous condensation on niobium nanoparticles. This combined mechanism makes nanoparticles to grow. In addition, the nanoparticles grow further by coagulation among themselves.

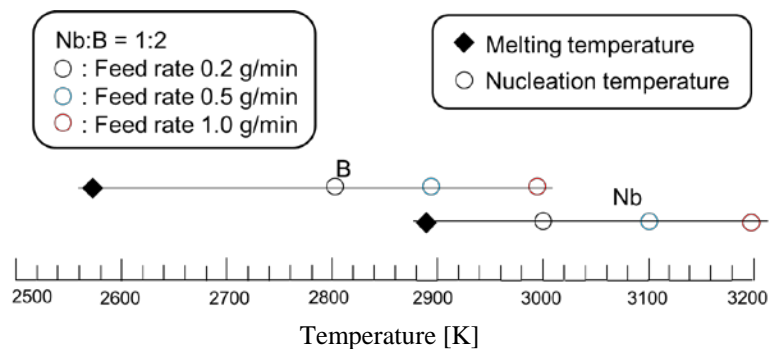


Figure 3. Nucleation temperature at the critical saturation ratio for constituent components of boride.

4. Results and Discussion

Figure 4 shows the XRD spectra of product at the fixed initial composition with different powder feed rates. From the XRD measurement, Nb and NbB₂ were identified. The dominant product was unreacted Nb, while the intensity of NbB₂ peaks was very low. This XRD result indicates that the synthesis of niobium boride nanoparticle is difficult compared with titanium borides [9]. The main reason of the little amount of prepared niobium boride is that the small temperature gap between the nucleation temperature and melting temperature of niobium. The nuclei on the liquid state are important in the formation of metal boride nanoparticles, because chemical reactions between Nb nuclei and B monomers are impossible after the solidification of Nb. Seen from figure 3, niobium nuclei in liquid state have relatively narrow region. The nucleation of niobium takes place only around the niobium nucleation temperature in a short time. Simultaneously, niobium and boron vapours co-condensate on the surface of niobium nuclei. During the high temperature region between the nucleation temperature and melting temperature of niobium, niobium and boron vapours can be mixed well on the liquid state. On the other hand, niobium and boron vapours are not mixed well in the relatively low temperature gap between the melting temperatures of niobium and boron. The relatively narrow temperature gap between the nucleation temperature and melting temperature of niobium means less boron and niobium vapours can be mixed well.

Figure 5 indicates the effect of powder feed rate on the phase composition of product. The mass fraction of niobium boride in the product decreases with increasing powder feed rate from the experimental results. Raw materials are fully evaporated in thermal plasma. With the low powder feed rate, both of boron and niobium are immediately evaporated when they are injected into the thermal plasma. Then the evaporated niobium is nucleated in a limited high temperature area at the upstream of plasma flow, where much niobium and boron co-exist and can react with each other. The amount of raw materials increases at high powder feed rate, though the heat from the plasma keeps constant at the fixed input power of 30.4 kW. The heat transferring from the plasma to each particle requires relatively long time in the case of high powder feed rate rather than the case of low one. In addition, niobium is difficult to be evaporated due to the relatively high melting temperature, evaporation

temperature, and latent heat. Therefore, the existence area of evaporated niobium is extended along with plasma flame. The boridation occurs easily in the upstream region of plasma flow due to high temperature and abundant boron vapour, while it is difficult in the downstream region because of relatively low temperature for the boridation and diffuse of boron vapour which is produced in the upstream region. Therefore, less niobium nuclei can react with boron, and the molar ratio of niobium boride nanoparticles in the product decreases at higher powder feed rate.

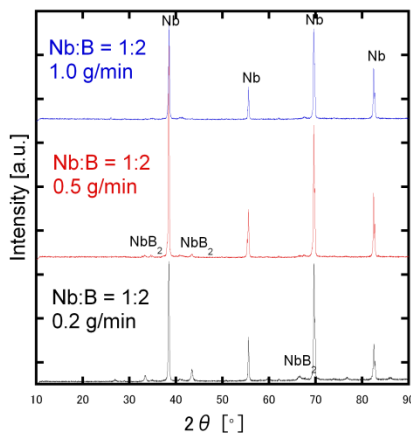


Figure 4. XRD spectra of product collected on the reactor wall at fixed initial composition with different powder feed rates.

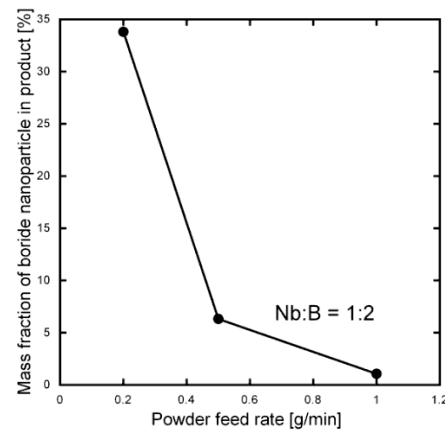


Figure 5. Effect of powder feed rate on the phase composition of product at Nb:B = 1:2.

Effect of powder feed rate on the crystalline diameter of as-prepared niobium boride nanoparticles is shown in figure 6. The crystalline size of the prepared nanoparticles increases along with powder feed rate. In high powder feed rate, the enhanced monomer density in the plasma leads to the high growth rate of niobium boride nanoparticles. In addition, the growth process including the nucleation and co-condensation processes occurs from the nucleation temperature of niobium to the melting temperature of boron. Based on figure 3, the growth time increases with powder feed rate. Furthermore, the nanoparticles are formed at earlier stage at the higher feed rate with relatively large amount of vapour compared with the case of low feed rate. For this reason the nucleation positions shift to the upstream region of plasma. Because the temperature in upstream is high, the nucleation rate of niobium is reduced. As a result, a small number of stable niobium nuclei which share a large amount of vapour are generated. Consequently, large size niobium boride nanoparticles are synthesized in the high feeding rate condition.

Figure 7 demonstrates the XRD spectra of products from the filter and the inner wall of the reaction chamber at the fixed niobium and boron composition of 1 to 3 with powder feed rate of 0.2 g/min. The dominant product from the filter is niobium boride, while the main product from the inner wall is unreacted niobium. Table 2 display the mass fraction of niobium boride in the product from the filter and the inner wall. The filter case has much higher mass fraction of niobium boride in the product than the inner wall case. In the reaction chamber, the high temperature region for the existence of niobium nuclei is limited in the centre region of the plasma flame due to the high melting temperature (2890 K) and boiling temperature (5120 K) of niobium. For this reason, the formation of niobium borides is difficult near the inner wall of the chamber because of the lower temperature. On the other hand, synthesized niobium borides in the centre region are transported to the filter along with plasma flow. Moreover, relatively low niobium boride density of 6.97 g/cm³ compared with niobium density of 8.57 g/cm³ promotes enhanced niobium boride fraction in the filter.

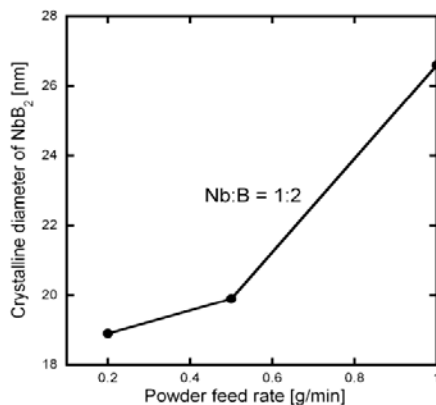


Figure 6. Effect of powder feed rate on the crystalline diameter of product at Nb:B = 1:2.

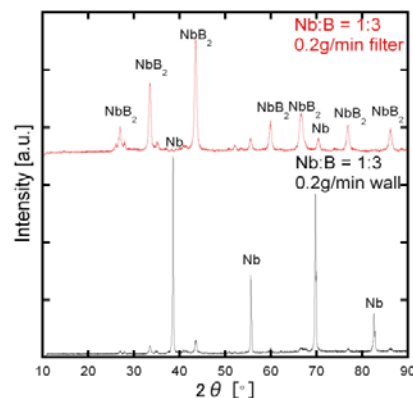


Figure 7. XRD spectrums of product from the filter and inner wall of chamber at the Nb:B = 1:3 with powder feed rate of 0.2 g/min.

Table 2 Mass fraction of niobium boride in the product from the filter and the inner wall of the reactor at the powder feed rate of 0.2 g/min.

Initial Composition	Filter (%)	Wall (%)
Nb:B = 1:2	96.66	33.81
Nb:B = 1:3	96.82	19.34
Nb:B = 1:4	96.75	16.88

5. Conclusions

Experimental study were carried out to prepare niobium boride nanoparticles and to investigate the effect of powder feed rate on the phase composition and crystalline size of product in RF thermal plasma. In this work, niobium boride nanoparticles were successfully synthesized in RF thermal plasma. The nucleation temperature plays an important role in the controlled synthesis of niobium boride nanoparticles in RF thermal plasma. The little production of niobium boride nanoparticles resulted from the relatively narrow temperature gap between the nucleation and melting temperatures of niobium. The mass fraction of niobium boride nanoparticles in the product was decreased with increasing the powder feed rate due to the extended evaporation region of raw materials. The crystalline size of niobium boride nanoparticles increased with the increase of powder feed rate. High mass fraction of the niobium boride nanoparticle in the product was found from the collecting filter due to high melting and boiling temperatures of niobium.

References

- [1] Watanabe T, Nezu A, Abe Y, Ishii Y and Adachi K 2003 *Thin Solid Films* **435** 27
- [2] Watanabe T and Okumiya H 2004 *Sci. Technol. Adv. Mater.* **5** 639
- [3] Szepvolgyi J, Markovic Z, Scheier P and Feil S 2006 *Plasma Chem. Plasma Process.* **26** 597
- [4] Shigeta M and Watanabe T 2005 *J. Mater. Res.* **20** 2801
- [5] Desilets M, Bilodeau JF and Proulx P 1997 *J. Phys. D: Appl. Phys.* **30** 1951
- [6] Gonzalez NYM, Morsli ME and Proulx P 2008 *J. Therm. Spray Technol.* **17** 533
- [7] Shigeta M and Watanabe T 2010 *J. Appl. Phys.* **108** 043306
- [8] Yeh CL, and Chen WH 2006 *J. Alloy Comp.* **422** 78
- [9] Cheng YY and Watanabe T 2011 *J. Chem. Eng. Jpn.* **44** 583
- [10] Shigeta M and Watanabe T 2009 *J. Therm. Spray Technol.* **18** 1022
- [11] Girshick SL, Chiu CP and McMurphy PH 1990 *Aerosol Sci. Technol.* **13** 465